Bulletin of Mathematical Biology (2020) 82:35
https://doi.org/10.1007/s11538-020-00711-4

Society for Mathematical Biology

ORIGINAL ARTICLE

Varying Inoculum Dose to Assess the Roles of the Immune Response and Target Cell Depletion by the Pathogen in Control of Acute Viral Infections

James R. Moore[1] · Hasan Ahmed[2] · Balaji Manicassamy[3] · Adolfo Garcia-Sastre[4] · Andreas Handel[5] · Rustom Antia[2]

Received: 21 December 2018 / Accepted: 19 February 2020

Abstract

It is difficult to determine whether an immune response or target cell depletion by the infectious agent is most responsible for the control of acute primary infection. Both mechanisms can explain the basic dynamics of an acute infection—exponential growth of the pathogen followed by control and clearance—and can also be represented by many different differential equation models. Consequently, traditional model comparison techniques using time series data can be ambiguous or inconclusive. We propose that varying the inoculum dose and measuring the subsequent infectious load can rule out target cell depletion by the pathogen as the main control mechanism. Infectious load can be any measure that is proportional to the number of infected cells, such as viraemia. We show that a twofold or greater change in infectious load is unlikely when target cell depletion controls infection, regardless of the model details. Analyzing previously published data from mice infected with influenza, we find the proportion of lung epithelial cells infected was 21-fold greater (95% confidence interval 14–32) in the highest dose group than in the lowest. This provides evidence in favor of an alternative to target cell depletion, such as innate immunity, in controlling influenza infections in this experimental system. Data from other experimental animal models of acute primary infection have a similar pattern.

Keywords Target cell depletion · Within-host modeling · Viral dynamics · Inoculum dose

This work was supported by three NIH Grants NIH U54GM111274, NIH R01AI110720, NIH U19AI11789102, (to R. Antia).

Electronic supplementary material The online version of this article (https://doi.org/10.1007/s11538-020-00711-4) contains supplementary material, which is available to authorized users.

✉ James R. Moore
jrmoore@fhcrc.org

Extended author information available on the last page of the article

Published online: 03 March 2020

1 Introduction

Acute infections are characterized by an initial period of growth followed by decline and eventually clearance. What explains the control of acute infections? It is well known that adaptive immunity generated by prior exposure to a pathogen can prevent or rapidly control subsequent infections with the same pathogen (Kreijtz et al. 2011). However, the situation may be different in primary infections of naive hosts. Experimental data, such as the data analyzed here (Manicassamy et al. 2010) as well as in other studies (Saenz et al. 2010; Carrat et al. 2008), show that the peak of the primary infections of naive hosts can be within a few days following inoculation. In these instances, the infection begins to decline substantially earlier than what might be expected if adaptive immunity were the main factor in controlling these infections (Doherty et al. 2006; Dobrovolny et al. 2013). This suggests that other factors such as target cell depletion by the virus or control of infection by innate immunity might be responsible for the initial control of primary infection with adaptive immunity becoming important some days later and helping to clear the infection.

In this paper, we define control of infection via pathogen-associated target cell depletion (CIPAT) to be the control of infection primarily due to the infectious agent killing enough of the available susceptible cells that it can no longer sustain itself. Target cells can also be depleted due to an immune response, but our analysis does not apply to this situation.

Acute viral infections often show a simple biphasic pattern: exponential growth followed by exponential decay, which is consistent with the target cell depletion hypothesis (Smith et al. 2010; Beauchemin and Handel 2011). Mathematical models with CIPAT as the primary mechanism of control have been used to represent the dynamics of HIV (Phillips 1996; Stafford et al. 2000; Perelson and Ribeiro 2013), SIV (Regoes et al. 2004), malaria (Antia et al. 2008; Haydon et al. 2003; Kochin et al. 2010), Zika (Best and Perelson 2018), West Nile (Banerjee et al. 2016), and influenza (Baccam et al. 2006; Petrie et al. 2013; Smith 2018). Therefore, establishing the role of CIPAT versus innate immunity in such infections is challenging, as mathematical models of CIPAT lacking an explicit immune response are often the simplest model that can reproduce the data. In this paper, we propose a simple method to establish evidence in favor of an alternative to CIPAT models, such as control by innate immunity.

Saenz et al. (2010) propose that the number of surviving target cells can potentially be used to provide evidence for the importance of innate immunity. They analyze data from influenza infection in ponies using both viral load data and a measure of lung epithelial cell depletion. They observe cell death of 27% of lung epithelial cells at the end of infection and argue that this level of target cell depletion is too low to explain the control of infection. Similarly, Myers et al. (2019) found active lesions in less than 50% of mouse lung tissue during influenza A infection. Although this method is useful for establishing evidence of immune control, it relies on an accurate measurement of the fraction of lung epithelial cells infected. Furthermore, it is possible that only a subset of lung epithelial cells are susceptible to infection (Dobrovolny et al. 2010). Therefore, data sets such as these cannot be readily used to provide evidence of innate immune control or any other alternative to CIPAT.

In this paper we build on Saenz et al. (2010) and Myers et al. (2019) by proposing a new method to establish evidence of an alternative to CIPAT. Li and Handel (2014) have shown that many models that fit the temporal dynamics of infection fail to reproduce the response to changes in inoculum dose. We show that models incorporating CIPAT are unable to reproduce large changes in the final size of infection with increasing inoculum dose. Therefore, the observation of any such large change can be viewed as evidence of the role of an alternative mechanism in viral control such as an innate immune response.

The results of this paper are organized as follows:

- For a large class of CIPAT models, there is a fixed relationship between size of infection and inoculum dose, dependent only on R_0.
- From this relationship we derive criteria for providing evidence for an alternative to CIPAT models: less than 50% of target cells become infected at low inoculum doses, or, equivalently, that there is a more than twofold change in infectious load when inoculum dose is varied.
- Applying these criteria to data from experimental influenza infection of mice Manicassamy et al. (2010) allows us to identify cases where there is evidence for an alternative to CIPAT.
- We show the general applicability of these results by applying the criterion to other studies of viral infection which varied the inoculum dose.

2 Results

2.1 Final Size for CIPAT Models

We define the final size (F) to be the total number of cells that become infected during an infection.

In this section, we will derive the final size predicted by CIPAT models (F_T) in terms of basic reproduction number R_0 and inoculum dose V_0. Similar formulas have been previously derived for epidemic models (Kermack and McKendrick 1927; Diekmann and Heesterbeek 2000; Ma and Earn 2006; Miller 2012), as well as for certain within-host models (Smith et al. 2010; Hadjichrysanthou et al. 2016). Here, we extend the reasoning of Miller (2012) to a larger class of within-host models.

The final size formula we derive applies to a large number of CIPAT models. One such model, from Baccam et al. (2006), is

$$\begin{aligned}\frac{\mathrm{d}V}{\mathrm{d}t} &= pI - cV\\ \frac{\mathrm{d}T}{\mathrm{d}t} &= -\beta TV\\ \frac{\mathrm{d}E}{\mathrm{d}t} &= \beta TV - kE\end{aligned}$$

$$\frac{\mathrm{d}I}{\mathrm{d}t} = kE - \delta I$$
$$V(0) = sD \quad T(0) = N \quad E(0) = 0 \quad I(0) = 0 \tag{1}$$

Here, V is the free virus, T is the number of susceptible target cells, E is the number of infected cells that do not produce virus, and I is the number of infected cells producing virus. The model assumes that during the timescale of the infection there is minimal replenishment of new target cells. The parameter p is the rate of production of virus from infected cells, c is the death rate of free virus, β represents infectivity and δ is the death rate of infected cells. The initial number of virions is linearly proportional to inoculum dose with proportionality constant s.

The final size is given by the following equation

$$1 - F_T/N = e^{-R_0(F_T/N + V_0/(NK))} \tag{2}$$

where $R_0 = p\beta N/(\delta c)$ is the basic reproduction number, V_0 is the size of the inoculum dose, and $K = p/b$ is the average number of virions produced per infected cell. In the limit as V_0 becomes very small, this result reduces to the final size shown in Smith et al. (2010).

Surprisingly, Eq. (2) still applies, with appropriate modifications for R_0 and K, even if we modify Eq. (1) to include more infectious stages or subpopulations of cells with different levels of infectivity, if we eliminate the eclipse phase, or if V is assumed to be in quasi-equilibrium with I. It also applies if the times that cells spend in each compartment are not exponentially distributed. See Ma and Earn (2006) or Miller (2012) for more details.

To derive Eq. (2) in a more generalized setting, we use the same formulation as Miller (2012), who considered epidemic models where the disease is spread via infected individuals. We extend this reasoning to explicitly include a separate viral compartment which spreads the disease, rather than infected cells themselves.

We make the following assumptions:

- There are a fixed number of cells N, i.e., new cells are not generated during the infection.
- An infected cell produces *on average* K virions over its infectious lifetime.
- Each virion has a probability P of infecting each susceptible cell.

The proportion of cells that do not get infected by the time the infection clears is $1 - F_T/N$. This proportion also represents the probability of a single cell remaining uninfected for the duration of infection. The probability of *not* being infected by each of V virions is, by assumption, $(1 - P)^V$. Therefore,

$$1 - F_T/N = (1 - P)^{V^*} \tag{3}$$

$V^* = KF_T + V_0$ is the total number of virions that must be evaded, where V_0 represents the inoculum dose and KF_T are all the additional virions produced by infected cells. Note that for the model represented by Eq. (1) $V^* = c\int_0^\infty V(t)\,\mathrm{d}t$. Plugging the definition for V^* into Eq. (3) yields

$$1 - F_T/N = (1 - P)^{KF+V_0} \tag{4}$$

We wish to rewrite the above equation using the parameter R_0 instead of P. By definition, R_0 is the number of secondary infections arising from a single cell, i.e., from K virions. Using similar reasoning as above, we derive $1 - R_0/N = (1 - P)^K$ and so

$$1 - F_T/N = \left(1 - \frac{R_0}{N}\right)^{F_T + V_0/K} \tag{5}$$

In the limit that N becomes very large, we derive Eq. (7)

$$1 - F_T/N = e^{-R_0(F_T/N + V_0/(NK))} \tag{6}$$

Solving for F_T yields

$$F_T(R_0, V_0) = N + \frac{N}{R_0} W\left[-R_0 e^{-R_0(1+V_0/(NK))}\right] \tag{7}$$

W is the upper branch of the Lambert W function.

2.2 Criteria for Establishing Immune Control

In this section, we use the final size equation (2) to identify experimental models of infection that are less likely to have CIPAT as a primary mechanism of control. We propose if the number of infected cells is observed to change by more than twofold when varying the inoculum dose, then the there is evidence of an alternative mechanism such as innate immunity.

Assuming target cell depletion by the pathogen controls infection, the final size F_T is insensitive to inoculum dose V_0, especially for large R_0 (Fig. 1a). For $R_0 > 1$, for example $R_0 = 1.4$, there will be a nonzero final size even as $V_0 \to 0$. If $R_0 \gg 1$, for example $R_0 = 5$, then even a very low dose is sufficient to infect almost all cells. If less than half the target cells become infected, then a CIPAT would predict $R_0 < 1.4$. For context we note that previous estimates for the within host R_0 of viruses include 3.5 and 22 for influenza (Hadjichrysanthou et al. 2016; Baccam et al. 2006), 8 for HIV (Perelson and Ribeiro 2013) and 30–35 for dengue (Clapham et al. 2014). In general the rapid growth rate of viruses during the initial phase of infection suggests high R_0. Therefore, less than 50% infection ($F/N < 0.5$) is provide evidence for an alternative to CIPAT.

Establishing that less than half of the target cells become infected may be impractical. First, it requires an accurate measure of the number of infected cells. Second, it requires knowing the number of susceptible cells. We therefore suggest a second criterion: the final size doubles when changing inoculum dose. Note that if $R_0 \leq 1$, then the final size is highly dependent on the inoculum dose. If $R_0 \gg 1$, then final size is relatively insensitive to inoculum dose as any nonzero dose will lead to a large number of cells becoming infected (see also Hadjichrysanthou et al. (2016)). By contrast if

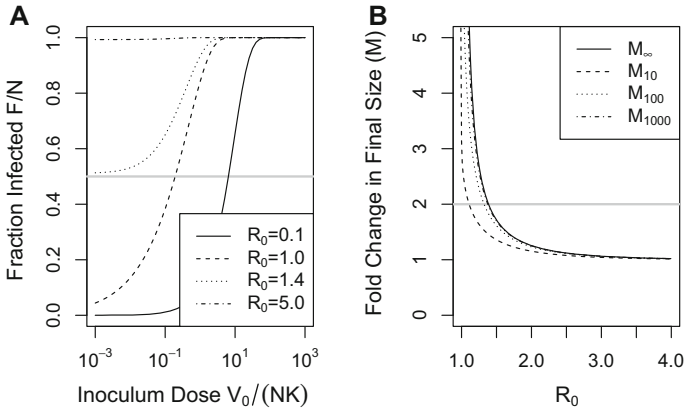

Fig. 1 Absolute and relative fraction infected. **a** The fraction of cells infected as a function of inoculum dose. **b** M versus R_0 in CIPAT models. M_x, the maximum fold change in final size due to x-fold changes in inoculum dose, is close to 1 in CIPAT model except at very low values of R_0. Hence, provided R_0 is not very small, a large variation in the final size from changes in inoculum dose provides evidence for an alternative to CIPAT. For example, greater than twofold variation is inconsistent with the model unless $R_0 < 1.4$

viral infection is controlled by an immune response, then a much smaller amount of target cells will be infected. For example, Myers et al. (2019) predict a final size of around 30% despite an R_0 of roughly 100, due to the role of CD8 T cells in controlling the infection.

For an experimental model of infection, let M_x be the maximum fold change in F due to an x-fold increase in the inoculum dose V_0. More precisely,

$$M_x = \max_{V_0} \left\{ \frac{F(xV_0)}{F(V_0)} \right\} \tag{8}$$

Let $M_{x,T}(R_0)$ be the maximum fold change for a CIPAT model with $F = F_T(R_0, V_0)$, such as Eq. (1). To establish evidence for an alternative to CIPAT, we must establish experimentally that $M_x > M_{x,T}(R_0)$. As F is only measured for a few values of V_0, any experimentally determined estimate, denoted by $\hat{M}_x$, will likely be an underestimate of M_x, therefore it suffices to show that $\hat{M}_x > M_{x,T}(R_0)$.

$M_{x,T}(R_0)$ decreases as R_0 increases—approaching 1 for higher values of R_0 (see Fig. 1). If we observe $\hat{M}_x \geq 2$, then CIPAT requires $R_0 \leq 1.4$. The greater the $\hat{M}_x$ observed, the more strict this R_0 condition becomes. For example, if $\hat{M}_x = 10$, then CIPAT requires that $R_0 \leq 1.06$. In general an observed fold change of $\hat{M}_x$ implies that,

$$R_0 \leq -\ln(1 - 1/\hat{M}_x)\hat{M}_x \tag{9}$$

Note that this criterion does not require an absolute measure of F. Instead we need only measure a value $L = \alpha F$ which is proportional to the final size. We shall refer to L as the infectious load. For example, if we use the AUC (area under the curve) of the viral load, then $L = F/(bc)$. When estimating $\hat{M}_x$ from data, we can use the

measured value L in the place of F as the fold change in the two quantities is the same. Therefore, $\hat{M}_x$ can be calculated even when F and α are not known.

2.3 CIPAT does not Explain Manicassamy Data

Manicassamy et al. (2010) quantified the effect of 1000-fold variation in the inoculum dose on the dynamics of influenza infection in mice. Here, we analyze their data along with previously unpublished data from the same experiment. Naive mice were infected with the influenza virus PR8 carrying a green fluorescent protein gene, and the proportion of lung epithelial cells that were influenza infected was measured. Three inoculum dose groups—10^4 PFU, 10^6 PFU and 10^7 PFU—were used. As these measurements require the killing of a mouse, only one time point is available for each individual.

Assuming infected cells have similar average life spans across the three dose groups, the final size is approximately proportional to the integral or area under the curve (AUC) of infected cells over time. Because the infection seems to be clearing by day 4 and because we only have data until day 4 for the 10^4 PFU and 10^7 PFU groups, we use an estimate of AUC over the first 4.5 days. Our infectious load is then

$$L \approx \int_{t=0}^{4.5\text{days}} I(t)\,\mathrm{d}t \approx t_{\text{inf}} F$$

where t_{inf} is the lifespan of an infected cell.

To use the first criterion, we have to estimate $F = L/t_{\text{inf}}$. Using data from infections of cell cultures, Beauchemin and Handel (2011) fit the infectious lifespan for influenza to be 12–48 h. As we are trying to establish an upper bound for the final size, we use 12 h in our calculations. Under this assumption, the lowest dose group has a final size of about 2.4% (95% confidence interval 1.6–3.3%) (Fig. 2b). This falls well short of the 50% threshold and suggests that $R_0 < 1.02$. However, this assumes that all lung epithelial cells are susceptible to infection. It also assumes all infected cells become fluorescent, when only a fraction do (Manicassamy et al. 2010). Using the same method, we estimate that 22.4% (17.1–28.0) and 50.9% (40.9–61.8) of target cells are infected in the 10^6 and 10^7 PFU groups, respectively.

Figure 2c shows the relative AUC (AUC / AUC for 10^4 PFU) by dose group. The AUC is much higher in the 10^7 PFU group as compared to the 10^4 PFU group (~ 21 fold difference, 95% confidence interval 14–32). The AUC in the 10^6 PFU group is also much higher than in the 10^4 PFU group (~ 9.1 fold difference, 95% confidence interval 6.1–14). Even taking the lower bound of $\hat{M}_{1000} = 14$, for this fold change to be possible under CIPAT requires $R_0 < 1.04$ according Eq. (9). This extremely low implied value of R_0 provides evidence for an alternative to CIPAT in this case.

2.4 Applying the Criterion to Other Data Sets

To test the generalizability of our results, we apply our criterion to a number of other studies of acute infection in which the inoculum dose was varied (Table 1). These

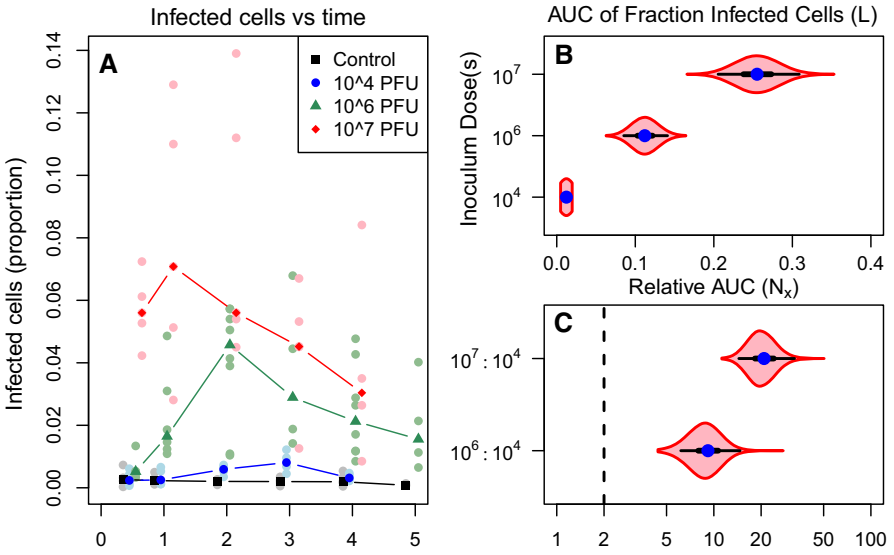

Fig. 2 Infectious load increases with inoculum dose. **a** The fraction of cells infected at each time point measured using green fluorescent protein (GFP). **b** We quantify infectious load with AUC (fraction infected cells over time). Horizontal bars show the 95% confidence intervals and inter-quartile range calculated from bootstrapped resamples. **c** The observed fold change N in the high and middle dose groups compared to the low dose group. We plot the relative AUC (AUC / AUC for the 10^4 PFU group) with 95% confidence intervals and inter-quartile range. The difference in AUC between the groups is statistically significant ($p < 0.001$ for all pairwise comparisons). This pattern, large variation in AUC with inoculum dose, is suggestive of control mechanisms other than CIPAT (Color figure online)

papers varied in the virus used, the host organisms, and the quantification method for infectious load. For each paper, we compared the infectious load at the highest and lowest inoculum dose to get a value for $\hat{M}_x$ (Fig. 3). Where error bars or raw data were included we calculated confidence intervals for these values. In all but one case the fold change in infectious load was greater than 2, indicating that the pattern seen in our data is not unusual for such experiments. Therefore, we expect to be able to rule out target cell limitation as the primary mechanism of control in many other experimental infections.

3 Discussion

Mathematical models have proved to be a useful tool for understanding the dynamics of virus infections (Perelson 2002) and have been widely applied to influenza infections (Baccam et al. 2006; Bocharov and Romanyukha 1994; Miao et al. 2010; Lee et al. 2009; Pawelek et al. 2016, 2012; Saenz et al. 2010; Cao et al. 2015; Smith et al. 2010; Canini and Carrat 2011; Canini et al. 2014; Zarnitsyna et al. 2016; Smith 2018; Smith et al. 2018; Myers et al. 2019), however these models often can reproduce the observed dynamics of infections with or without an immune response. In this paper we focus on distinguishing between target cell depletion by the pathogen alone (CIPAT)

Table 1 Other studies of inoculum dose

Study	Infection (host)	Dose range	Measure
Ginsberg and Horsfall (1952)	Influenza A (mice)	$10^{-2.6}-10^{2.4}$ Units	Viral Titer in lungs
Iida and Bang (1963)	Influenza A (mice)	$10^{5.5}-10^{7.5}$ EID_{50}	EID_{50} in nasal tissue
Prince et al. (1993)	Adenovirus (cotton rats)	$10^{6}-10^{7}$ PFU	FFU in lungs
Ottolini et al. (1996)	Parainfluenza (cotton rats)	$10^{1.5}-10^{5.5}$ PFU	PFU in lungs
Ottolini et al. (2005)	Influenza A (cotton rats)	$10^{3}-10^{7}$ $TCID_{50}$	$TCID_{50}$ in lungs
Callison et al. (2006)	Bronchitis (chickens)	$10^{1.2}-10^{5.2}$ EID_{50}	Genomes in trachea
Liu et al. (2009)	Norovirus (mice)	$10^{3}-10^{7}$ PFU	PFU in intestines

A selection of other papers that have measured the change in infectious load in response to changing inoculum dose. The 'measure' column is the infectious load definition used in the study (*FFU* fluorescent focus units)

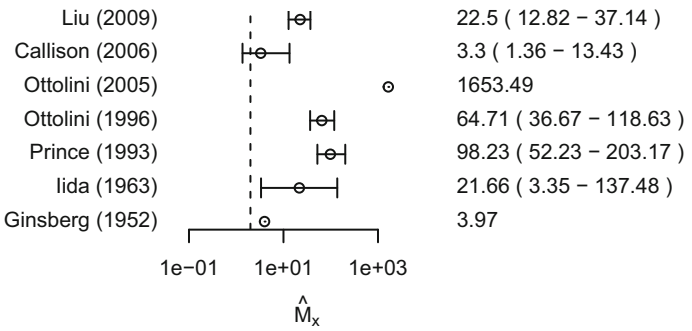

Fig. 3 Fold changes in other studies. We calculate the fold change in the infectious load due to inoculum dose (M) from a number of other studies. The dashed line shows are cutoff of $M = 2$. In many cases, the value of M is too high to be explained by CIPAT

and other mechanisms of control. We suggest that a two fold increase in infectious load with increase in inoculum dose provides evidence for an alternative to CIPAT, as this implies that R_0 must be very low. Infectious load is any measure that is expected to correlate with the total number of cells that become infected over the course of infection. This could be, for example, the area under the curve (AUC) of number of infected cells or even of viral load. We show that this criterion applies to a wide class of CIPAT models, including the models used by Baccam et al. (2006).

We also examine data from Manicassamy et al. (2010). We first show that based on our criterion these data are inconsistent with CIPAT, as there is a very large fold change in infectious load with increasing inoculum dose. Other animal models of acute viral infection also show dramatic changes in infectious load due to inoculum dose. The pattern is seen in infection models of influenza (Ginsberg and Horsfall 1952; Iida and Bang 1963; Ottolini et al. 2005), parainfluenza (Ottolini et al. 1996), adenovirus (Prince et al. 1993), foot and mouth disease (Quan et al. 2004), and norovirus (Liu et al. 2009). Therefore, we expect to be able to rule out CIPAT as the primary mechanism of clearance in many acute infections.

This work has a number of assumptions and corresponding caveats. We assume that the basic reproductive number of the infection R_0 is not very low, the system is well mixed (see Beauchemin 2006; Ma and Earn 2006; Keeling and Rohani 2008 for a discussion of spatial structure), and the number of target cells is not replenished during the timescale of the infection. There are other limitations that pertain to the data used for our analysis. Our data come from infection of mice with a single strain of influenza. It is also likely that GFP expression underestimated the number of infected cells; comparison of GFP and influenza nucleoprotein expression for the 10^6 PFU group showed very similar trajectories albeit with GFP expression consistently showing fewer infected cells. As we do not expect the degree of undercount to vary substantially by group, we expect the results of our analysis to hold. We note that our analysis does not apply to all possible models of CIPAT. For example, it does not include models with heterogeneity in susceptibility. It is also likely that at higher inoculum doses than those tested here, target cell limitation does become the primary mechanism of clearance.

Mathematical models of within host dynamics of infection have multiple uses. For one, they can aid our understanding of the underlying biology by testing hypotheses against the data. They can also be used to make predictions about the dynamics of a disease in new hosts. Li and Handel (2014) demonstrated that many of these models can predict the temporal dynamics of acute viral infection, but fail to reproduce even the qualitative response to changing inoculum dose. Therefore, we can refine our models and learn about the underlying biology of infection using data from such experiments. Target cell depletion models are used in a variety of contexts (Baccam et al. 2006; Beauchemin and Handel 2011; Smith et al. 2013; Elemans et al. 2011; Banerjee et al. 2016; Best et al. 2017; Best and Perelson 2018; Hill et al. 2018) as they provide a good fit to the data with a relatively simple model. However, they may not be a good representation of the underlying biology and consequently may not make good predictions in some contexts. Here, we show that target cell depletion models fail to predict the change in infection dynamics with a changing inoculum dose that is frequently observed in experimental systems.

4 Methods

4.1 Experimental Data

The experimental data come from a previously published study augmented with previously unpublished data from the same experiment. See Manicassamy et al. (2010) for details and supplement S1 for the data. Mice were infected with PR8 viruses with a modified NS1 gene fused to GFP. This allowed the proportion of infected lung epithelial cells to be measured by looking for GFP expression. Doses given were $\mathbf{D} = \{0, 10^4, 10^6, 10^7\}$ PFU and the virus was measured on days $\mathbf{t} = \{.5, 1, 2, 3, 4, 5\}$ post-infection. Each combination of dose and time point was used except for day 5 post-infection, when only the control ($D = 0$) and intermediate ($D = 10^6$) treatments were recorded.

We shall refer to G_{ijk} as the fraction of infected cells (as measured by GFP), in the kth mouse that received the D_ith dose, measured on the t_jth day post-infection.

4.2 Calculation of AUC

To calculate AUCs from the data, we noted that even if the inoculum dose is zero, the recorded number of infected cells, I, is greater than zero. To adjust for this background GFP expression, we calculated

$$G_{\text{Back}} = \sum_{j\in\mathbf{t}} \sum_{k=1}^{n_{1j}} G_{1jk} / \sum_{j\in\mathbf{t}} n_{1j} \tag{10}$$

where n_{1j} is the number measurements for the control group on the jth day.

AUC for the first 4.5 days was calculated using a nearest neighbor rectangle method, i.e.,

$$AUC_i = \sum_j w_j \sum_{k=1}^{n_{ij}} (G_{ijk} - G_{\text{Back}})/n_{ij} \tag{11}$$

where n_{ij} is the number of mice with $D = i$ and $t = j$ and $\mathbf{w} = \{0.75, 0.75, 1, 1, 1\}$ are the weights for the rectangle method. Confidence intervals for the AUCs were calculated via bootstrap with the *R* package 'boot' using 10000 resamples. For each i and j, the n_{ij} mice in each group were resampled with replacement and the AUC, as well as the relative AUC between groups, was recalculated.

5 Supporting Information

S1 File Data analyzed in this study.

Acknowledgements We thank Beth Kochin for insightful observations.

References

Antia R, Yates A, de Roode JC (2008) The dynamics of acute malaria infections. I. Effect of the parasite's red blood cell preference. Proc R Soc Lond B Biol Sci 275(1641):1449–1458. https://doi.org/10.1098/rspb.2008.0198

Baccam P, Beauchemin C, Macken CA, Hayden FG, Perelson AS (2006) Kinetics of influenza A virus infection in humans. J Virol 80(15):7590–7599. https://doi.org/10.1128/JVI.01623-05

Banerjee S, Guedj J, Ribeiro RM, Moses M, Perelson AS (2016) Estimating biologically relevant parameters under uncertainty for experimental within-host murine west nile virus infection. J R Soc Interface 13(117):20160130

Beauchemin C (2006) Probing the effects of the well-mixed assumption on viral infection dynamics. J Theor Biol 242(2):464–477. https://doi.org/10.1016/j.jtbi.2006.03.014

Beauchemin CA, Handel A (2011) A review of mathematical models of influenza A infections within a host or cell culture: lessons learned and challenges ahead. BMC Public Health. https://doi.org/10.1186/1471-2458-11-S1-S7

Best K, Perelson AS (2018) Mathematical modeling of within-host zika virus dynamics. Immunol Rev 285(1):81–96

Best K, Guedj J, Madelain V, de Lamballerie X, Lim SY, Osuna CE, Whitney JB, Perelson AS (2017) Zika plasma viral dynamics in nonhuman primates provides insights into early infection and antiviral strategies. PNAS 114(33):8847–8852

Bocharov G, Romanyukha A (1994) Mathematical model of antiviral immune response III. Influenza A virus infection. J Theor Biol 167(4):323–360. https://doi.org/10.1006/jtbi.1994.1074

Callison SA, Hilt DA, Boynton TO, Sample BF, Robison R, Swayne DE, Jackwood MW (2006) Development and evaluation of a real-time Taqman RT-PCR assay for the detection of infectious bronchitis virus from infected chickens. J Virol Methods 138(1):60–65

Canini L, Carrat F (2011) Population modeling of influenza A/H1N1 virus kinetics and symptom dynamics. J Virol 85(6):2764–2770. https://doi.org/10.1128/JVI.01318-10

Canini L, Conway JM, Perelson AS, Carrat F (2014) Impact of different oseltamivir regimens on treating influenza A virus infection and resistance emergence: insights from a modelling study. PLoS Comput Biol 10(4):e1003568. https://doi.org/10.1371/journal.pcbi.1003568

Cao P, Yan AW, Heffernan JM, Petrie S, Moss RG, Carolan LA, Guarnaccia TA, Kelso A, Barr IG, McVernon J, Laurie KL, McCaw JM (2015) Innate immunity and the inter-exposure interval determine the dynamics of secondary influenza virus infection and explain observed viral hierarchies. PLoS Comput Biol 11(8):e1004334. https://doi.org/10.1371/journal.pcbi.1004334

Carrat F, Vergu E, Ferguson NM, Lemaitre M, Cauchemez S, Leach S, Valleron AJ (2008) Time lines of infection and disease in human influenza: a review of volunteer challenge studies. Am J Epidemiol 167(7):775–785. https://doi.org/10.1093/aje/kwm375

Clapham HE, Tricou V, Chau NVV, Simmons CP, Ferguson NM (2014) Within-host viral dynamics of dengue serotype 1 infection. J R Soc Interface 11(96):20140094. https://doi.org/10.1098/rsif.2014.0094

Diekmann O, Heesterbeek JAP (2000) Mathematical epidemiology of infectious diseases: model building, analysis and interpretation, vol 5. Wiley, New York

Dobrovolny HM, Baron MJ, Gieschke R, Davies BE, Jumbe NL, Beauchemin CA (2010) Exploring cell tropism as a possible contributor to influenza infection severity. PLoS ONE 5(11):e13811. https://doi.org/10.1371/journal.pone.0013811

Dobrovolny HM, Reddy MB, Kamal MA, Rayner CR, Beauchemin CA (2013) Assessing mathematical models of influenza infections using features of the immune response. PLoS ONE 8(2):e57088. https://doi.org/10.1371/journal.pone.0057088

Doherty PC, Turner SJ, Webby RG, Thomas PG (2006) Influenza and the challenge for immunology. Nat Immunol 7(5):449–455. https://doi.org/10.1038/ni1343

Elemans M, Thiébaut R, Kaur A, Asquith B (2011) Quantification of the relative importance of CTL, B cell, NK cell, and target cell limitation in the control of primary SIV-infection. PLoS Comput Biol 7(3):e1001103

Ginsberg HS, Horsfall FL (1952) Quantitative aspects of the multiplication of influenza a virus in the mouse lung relation between the degree of viral multiplication and the extent of pneumonia. J Exp Med 95(2):135–145. https://doi.org/10.1084/jem.95.2.135

Hadjichrysanthou C, Cauet E, Lawrence E, Vegvari C, de Wolf F, Anderson RM (2016) Understanding the within-host dynamics of influenza A virus: from theory to clinical implications. J R Soc Interface 13(119):20160289. https://doi.org/10.1098/rsif.2016.0289

Haydon DT, Matthews L, Timms R, Colegrave N (2003) Top-down or bottom-up regulation of intra-host blood-stage malaria: do malaria parasites most resemble the dynamics of prey or predator? Proc R Soc Lond B Biol Sci 270(1512):289–298. https://doi.org/10.1098/rspb.2002.2203

Hill AL, Rosenbloom DI, Nowak MA, Siliciano RF (2018) Insight into treatment of HIV infection from viral dynamics models. Immunol Rev 285(1):9–25

Iida T, Bang FB (1963) Infection of the upper respiratory tract of mice with influenza A virus. Am J Hyg 77(2):169–76

Keeling MJ, Rohani P (2008) Modeling infectious diseases in humans and animals. Princeton University Press, Princeton

Kermack WO, McKendrick AG (1927) A contribution to the mathematical theory of epidemics. Proc R Soc Lond A 115(772):700–721

Kochin BF, Yates AJ, De Roode JC, Antia R (2010) On the control of acute rodent malaria infections by innate immunity. PLoS ONE 5(5):e10444. https://doi.org/10.1371/journal.pone.0010444

Kreijtz J, Fouchier R, Rimmelzwaan G (2011) Immune responses to influenza virus infection. Virus Res 162(1–2):19–30. https://doi.org/10.1016/j.virusres.2011.09.022

Lee HY, Topham DJ, Park SY, Hollenbaugh J, Treanor J, Mosmann TR, Jin X, Ward BM, Miao H, Holden-Wiltse J, Perelson AS, Zand M, Wu H (2009) Simulation and prediction of the adaptive immune response to influenza A virus infection. J Virol 83(14):7151–7165. https://doi.org/10.1128/JVI.00098-09

Li Y, Handel A (2014) Modeling inoculum dose dependent patterns of acute virus infections. J Theor Biol 347:63–73. https://doi.org/10.1016/j.jtbi.2014.01.008

Liu G, Kahan SM, Jia Y, Karst SM (2009) Primary high-dose murine norovirus 1 infection fails to protect from secondary challenge with homologous virus. J Virol 83(13):6963–6968

Ma J, Earn DJ (2006) Generality of the final size formula for an epidemic of a newly invading infectious disease. Bull Math Biol 68(3):679–702. https://doi.org/10.1007/s11538-005-9047-7

Manicassamy B, Manicassamy S, Belicha-Villanueva A, Pisanelli G, Pulendran B, García-Sastre A (2010) Analysis of in vivo dynamics of influenza virus infection in mice using a GFP reporter virus. PNAS 107(25):11531–11536. https://doi.org/10.1073/pnas.0914994107

Miao H, Hollenbaugh JA, Zand MS, Holden-Wiltse J, Mosmann TR, Perelson AS, Wu H, Topham DJ (2010) Quantifying the early immune response and adaptive immune response kinetics in mice infected with influenza A virus. J Virol 84(13):6687–6698. https://doi.org/10.1128/JVI.00266-10

Miller JC (2012) A note on the derivation of epidemic final sizes. Bull Math Biol 74(9):2125–2141. https://doi.org/10.1007/s11538-012-9749-6

Myers MA, Smith AP, Lane LC, Moquin DJ, Michael R, Vogel P, Woolard S, Smith AM (2019) The nonlinear relations that predict influenza viral dynamics, CD8+ T cell-Mediated Clearance, lung pathology, and disease severity. bioRxiv p 555276

Ottolini MG, Porter DD, Hemming VG, Hensen SA, Sami IR, Prince GA (1996) Semi-permissive replication and functional aspects of the immune response in a cotton rat model of human parainfluenza virus type 3 infection. J Gen Virol 77(8):1739–1743

Ottolini MG, Blanco JC, Eichelberger MC, Porter DD, Pletneva L, Richardson JY, Prince GA (2005) The cotton rat provides a useful small-animal model for the study of influenza virus pathogenesis. J Gen Virol 86(10):2823–2830

Pawelek KA, Huynh GT, Quinlivan M, Cullinane A, Rong L, Perelson AS (2012) Modeling within-host dynamics of influenza virus infection including immune responses. PLoS Comput Biol 8(6):e1002588. https://doi.org/10.1371/journal.pcbi.1002588

Pawelek KA, Dor D Jr, Salmeron C, Handel A (2016) Within-host models of high and low pathogenic influenza virus infections: the role of macrophages. PLoS ONE 11(2):e0150568. https://doi.org/10.1371/journal.pone.0150568

Perelson AS (2002) Modelling viral and immune system dynamics. Nat Rev Immunol 2(1):28–36. https://doi.org/10.1038/nri700

Perelson AS, Ribeiro RM (2013) Modeling the within-host dynamics of HIV infection. BMC Biol 11(1):96. https://doi.org/10.1186/1741-7007-11-96

Petrie SM, Guarnaccia T, Laurie KL, Hurt AC, McVernon J, McCaw JM (2013) Reducing uncertainty in within-host parameter estimates of influenza infection by measuring both infectious and total viral load. PLoS ONE 8(5):e64098

Phillips AN (1996) Reduction of HIV concentration during acute infection: independence from a specific immune response. Science 271(5248):497. https://doi.org/10.1126/science.271.5248.497

Prince G, Porter D, Jenson AB, Horswood R, Chanock R, Ginsberg H (1993) Pathogenesis of adenovirus type 5 pneumonia in cotton rats (sigmodon hispidus). J Virol 67(1):101–111

Quan M, Murphy C, Zhang Z, Alexandersen S (2004) Determinants of early foot-and-mouth disease virus dynamics in pigs. J Comp Pathol 131(4):294–307

Regoes RR, Antia R, Garber DA, Silvestri G, Feinberg MB, Staprans SI (2004) Roles of target cells and virus-specific cellular immunity in primary simian immunodeficiency virus infection. J Virol 78(9):4866–4875. https://doi.org/10.1128/JVI.78.9.4866-4875.2004

Saenz RA, Quinlivan M, Elton D, Macrae S, Blunden AS, Mumford JA, Daly JM, Digard P, Cullinane A, Grenfell BT, McCauley JW, Wood JL, Gog JR (2010) Dynamics of influenza virus infection and pathology. J Virol 84(8):3974–3983. https://doi.org/10.1128/JVI.02078-09

Smith AM (2018) Host-pathogen kinetics during influenza infection and coinfection: insights from predictive modeling. Immunol Rev 285(1):97–112

Smith AM, Adler FR, Perelson AS (2010) An accurate two-phase approximate solution to an acute viral infection model. J Math Biol 60(5):711–726. https://doi.org/10.1007/s00285-009-0281-8

Smith AM, Adler FR, Ribeiro RM, Gutenkunst RN, McAuley JL, McCullers JA, Perelson AS (2013) Kinetics of coinfection with influenza A virus and streptococcus pneumoniae. PLoS Pathog 9(3):e1003238

Smith AP, Moquin DJ, Bernhauerova V, Smith AM (2018) Influenza virus infection model with density dependence supports biphasic viral decay. Front Microbiol 9:1554

Stafford MA, Corey L, Cao Y, Daar ES, Ho DD, Perelson AS (2000) Modeling plasma virus concentration during primary HIV infection. J Theor Biol 203(3):285–301. https://doi.org/10.1006/jtbi.2000.1076

Zarnitsyna VI, Lavine J, Ellebedy A, Ahmed R, Antia R (2016) Multi-epitope models explain how pre-existing antibodies affect the generation of broadly protective responses to influenza. PLoS Pathog 12(6):e1005692. https://doi.org/10.1371/journal.ppat.1005692

Affiliations

James R. Moore[1] · Hasan Ahmed[2] · Balaji Manicassamy[3] · Adolfo Garcia-Sastre[4] · Andreas Handel[5] · Rustom Antia[2]

1 Division of Vaccines and Infectious Diseases, Fred Hutchinson Cancer Research Center, Seattle, USA

2 Department of Biology, Emory University, Atlanta, USA

3 Department of Microbiology and Immunology, University of Iowa School College of Medicine, Iowa City, USA

4 Department of Microbiology, Mt Sinai School of Medicine, New York, USA

5 Epidemiology and Biostatistics, University of Georgia, Athens, USA